# Efficient PHY Layer Abstraction for 5G NR Sidelink in ns-3

Liu Cao\* University of Washington Seattle, Washington, USA liucao@uw.edu Lyutianyang Zhang\* University of Washington Seattle, Washington, USA lyutiz@uw.edu Sumit Roy University of Washington Seattle, Washington, USA sroy@uw.edu

### **ABSTRACT**

Physical (PHY) layer abstraction is an effective method to reduce the runtimes compared with link simulations but still accurately characterize the link performance. As a result, PHY layer abstraction for IEEE 802.11 WLAN and 3GPP LTE/5G has been widely configured in the network simulators such as ns-3, which achieve faster systemlevel simulations quantifying the network performance. Since the first publicly accessible 5G NR Sidelink (SL) link simulator has been recently developed, it provides a possibility of implementing the first PHY layer abstraction on 5G NR SL. This work deploys an efficient PHY layer abstraction method (i.e., EESM-log-SGN) for 5G NR SL based on the offline NR SL link simulation. The obtained layer abstraction which is further stored in ns-3 for use aims at the common 5G NR SL scenario of OFDM unicast single layer mapping in the context of Independent and Identically Distributed (i.i.d.) frequency-selective channels. We provide details about implementation, performance, and validation.

### **CCS CONCEPTS**

• Computing methodologies → Modeling and Simulation; *Model verification and validation.* 

## **KEYWORDS**

Network Simulator 3 (ns-3), 5G NR, Sidelink, PHY Layer Abstraction, EESM-log-SGN, TB BLER, Numerology

# ACM Reference Format:

Liu Cao, Lyutianyang Zhang, and Sumit Roy. 2023. Efficient PHY Layer Abstraction for 5G NR Sidelink in ns-3. In 2023 Workshop on ns-3 (WNS3 2023), June 28–29, 2023, Arlington, VA, USA. ACM, New York, NY, USA, 6 pages. https://doi.org/10.1145/3592149.3592163

## 1 INTRODUCTION

As 5G New Radio (NR) Sidelink (SL) has been specified in Release 16 by the Third Generation Partnership Project (3GPP), researchers have been expressing increasing interest in SL in various research areas, such as Proximity Services (ProSe) [1] and Vehicle-to-Everything (V2X) [2]. It is essential to provide researchers with a comprehensive

Permission to make digital or hard copies of part or all of this work for personal or classroom use is granted without fee provided that copies are not made or distributed for profit or commercial advantage and that copies bear this notice and the full citation on the first page. Copyrights for third-party components of this work must be honored. For all other uses, contact the owner/author(s).

WNS3 2023, June 28–29, 2023, Arlington, VA, USA

© 2023 Copyright held by the owner/author(s).

ACM ISBN 979-8-4007-0747-6/23/06.

https://doi.org/10.1145/3592149.3592163

Table 1: Runtimes for 40000-TB Simulation at One SNR Point under 5G NR SL OFDM Unicast Single Transmission Scenario Using NIST 5G NR SL Simulator on Intel Core i7 CPU at 2.60GHz

$n_t \times n_r$	Numerology	# of RBs	Full PHY
1 × 1	0	10	48 min
1 × 1	0	20	56 min
1 × 1	1	10	57 min
1 × 1	1	20	62 min
$2 \times 2$	0	10	89 min
$2 \times 2$	0	20	108 min
$2 \times 2$	1	10	111 min
$2 \times 2$	1	20	156 min

simulation platform that allows for extensive NR SL link-level evaluations [20]. The first publicly accessible 5G NR SL link simulator<sup>1</sup>, which was developed by the National Institute of Standards and Technology (NIST), is a MATLAB-based simulator that complies with the 3GPP 5G NR SL standards [3–8] and offers flexible control over various Physical (PHY) layer configurations. The current NIST 5G NR SL link simulator supports Orthogonal Frequency Division Multiplexing (OFDM) Unicast Single/Hybrid Automatic Repeat Request (HARQ) transmission cases with focusing on Physical SL Shared Channel (PSSCH), i.e., assuming perfect Physical SL Control Channel (PSCCH). The inherited features from Vienna NR Uplink (UL)/Downlink (DL) link simulator <sup>2</sup> and MathWorks 5G toolbox provide general functionalities to the NR SL implementation [20].

Full PHY (link) simulations running on the NIST 5G NR SL link simulator, obtain packet performance at a single receiver, using runtime-costly symbol-level simulation of the PHY layer [16]. As shown in Table 1, the average runtimes of a full PHY simulation for 40000 transport blocks (TBs) <sup>3</sup> under different setups on a single OFDM link may require upto hour-long runtimes. This results from the need for generating complete channel realizations and transceiver signal processing within a full PHY simulation. Meanwhile, even the state-of-the-art PHY layer abstraction <sup>4</sup> aimed at

<sup>\*</sup>Both authors contributed equally to this work.

 $<sup>^1{\</sup>rm The~NIST~5G~NR~SL}$  link simulator can be found at: https://www.nist.gov/services-resources/software/new-radio-sidelink-simulator.

 $<sup>^2{\</sup>rm The\ Vienna}$ 5G link simulator can be found at: https://www.tuwien.at/etit/tc/vienna-simulators/vienna-5g-simulators/.

<sup>&</sup>lt;sup>3</sup>According to [21],  $n \ge \frac{400(1-\text{BLER}avg)}{\text{BLER}avg}$  can achieve the accuracy bound  $Pr\left[\left|\frac{1}{n}\sum_{i=1}^{n}X_{i}-\text{BLER}avg\right| \le 0.1\text{BLER}avg\right] \ge 0.95$ , where the sample mean  $\frac{1}{n}\sum_{i=1}^{n}X_{i}$  is used as an estimator of the average TB BLER, and  $X_{i} \in \{0,1\}$  is the binary TB error state of the i-th TB and n is the number of TBs. Thus, at least 40000-TB runs are required to accurately estimate the TB BLER down to around  $10^{-2}$  for each PHY setup [22].

<sup>&</sup>lt;sup>4</sup>The PHY layer abstraction is an equivalent packet error model for successful/unsuccessful MAC PDU reception based on the underlying PHY layer setup for use in ns-3 [10].

IEEE 802.11 WLAN and 3GPP UL/DL [13, 17–19, 21] implemented within the link-2-system (L2S) mapping workflow for reducing ns-3 runtimes, still scale as system dimensionality and node complexity increase.

In prior work, an efficient PHY layer abstraction method based on EESM-log-SGN approximation for the effective SNR at receiver output for Orthogonal Frequency Division Multiplexing/Multiple Access (OFDM/OFDMA) modulation for single or multi-user Multi-Input Multi-Output (MIMO) systems has been developed, and shown to require modest storage with runtimes insensitive to PHY layer dimensionality [16]. This PHY abstraction effort was developed and applied to MIMO WiFi and to the best of our knowledge, similar efficient PHY layer abstraction for 5G NR SL has not been implemented due to the lack of a commercial NR SL link simulator <sup>5</sup>.

This work sets an initial goal for NR SL PHY layer abstraction in ns-3, by customizing the EESM-log-SGN PHY workflow [16] using the (publicly accessible) NIST 5G NR SL simulator. Note that the base EESM-log-SGN method has been shown to be effective for independent and identically distributed (i.i.d.) tapped delay line (TDL) implementations of frequency-selective channels impacting OFDM/OFDMA. We demsontrate that the EESM-log-SGN method can be applied for 3GPP defined Pedestrian-B channel model for SL. While this is consistent with the NIST simulator that presently only supports i.i.d. channel instances, it is clear that low mobility (pedestrian) channels correlate over time and the current abstraction approach is inadequate. Future PHY abstraction work will target incorporation of temporal channel variations using the EESM-log-AR method [15].

The rest of the paper is organized as follows. In Section 2, we present a complement EESM-log-SGN framework for the 5G NR SL based on the full PHY from the NIST SL link simulator. Section 3 shows multiple simulation results using the simulator to verify the EESM-log-SGN framework. Finally, Section 4 draws our concluding remarks for this paper.

# 2 PHY LAYER ABSTRACTION FOR 5G NR SL

In this section, we present an efficient PHY layer abstraction model for 5G NR SL PHY layer that characterizes accurate end-2-end link performance (instantaneous TB BLER). The workflow in Figure 2 is required to implement the EESM-log-SGN PHY layer abstraction, consisting of offline link simulation whose results, captured via look-up tables (LUT) are made available at runtime for network simulation. The offline link simulation is conducted using the NIST 5G NR SL link simulator that provides calibrated Link-to-System (L2S) mapping parameters via model-fitting via the EESM-log-SGN method. The stored EESM-log-SGN parameters are used at runtime within ns-3 to generate the representative link performance for the PHY in support of a scheduled MAC transmission.

In the NR SL link simulator, the frequency-selective channel instance is assumed to be invariant during each transport block (TB) transmission over a slot <sup>6</sup> and different TB transmissions have different channel instances. Figure 1 shows an example of such frequency-selective block fading channels used in our simulation, where the

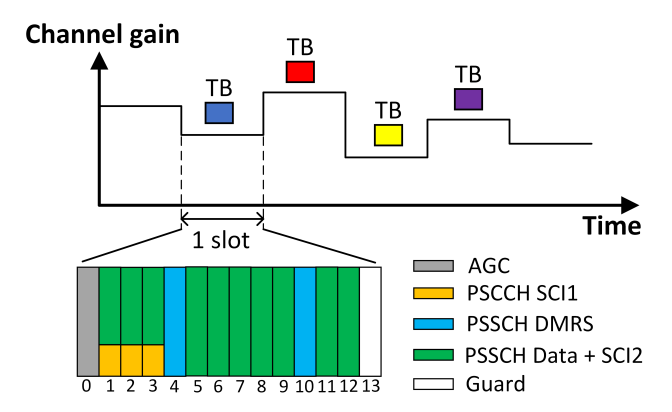


Figure 1: Frequency-selective Block Fading Channel for Single Transmission Case in the NIST 5G NR SL Simulator

deployed NR SL channel model is Pedestrian-B following the ITU standard [14]. For the considered block fading channel, the Doppler shift is assumed to be very small such that inter-carrier interference can be ignored <sup>7</sup>. Noise at each receiver is assumed to be AWGN, with identical power over different resource blocks (RBs). The PHY layer abstraction is aimed at the single transmission case where the Physical SL Feedback Channel (PSFCH) is disabled in the SL slot [20] and all available resource elements (REs) are utilized for the mapping of PSSCH data.

The flowchart of implementing the PHY layer abstraction for the 5G NR SL is shown in Figure 2. In the link simulation part of the implementation, a full PHY simulation is first conducted to obtain the post-processing SINR matrix and the associated binary TB error state (1(0) indicates TB error (success), respectively) for each TB. In a general SL system, suppose I spatial streams (information flows) are sent from the transmitter UE to the receiver UE using the set of resource blocks  $\mathcal{N}$ . A general expression for the post-processing SINR at the receiver's nth ( $n \in \mathcal{N}$ ) RB and ith ( $i \in I$ ) stream, SINR $_{i,n}$ , is given by:

$$SINR_{i,n} = \frac{S_{i,n}}{I_{i,n}^{s} + I_{i,n}^{o} + N_{i,n}},$$
(1)

where  $S_{i,n}$  is the received signal power,  $I_{i,n}^s$  is the inter-stream interference,  $I_{i,n}^o$  is the interference from other interferers, and  $N_{i,n}$  is the noise power. In this work, we consider only the single transmission between two UEs using the single layer mapping (i.e., single stream, |I|=1) without other interfering UEs, hence  $I_{1,n}^s=I_{1,n}^o=0$ . The corresponding post-processing SINR at the nth RB, SINR<sub>1,n</sub>, is [19]:

$$SINR_{1,n} = \frac{S_{1,n}}{N_{1,n}}.$$
 (2)

Computing the SINR in (2) requires the signal power  $S_{1,n}$  and noise power  $N_{1,n}$  at the n-th RB (i.e. frequency domain), whereas the SL simulator only provides estimates in the time domain. By applying Fast Fourier Transform (FFT) method, denoted by  $\mathcal{F}\{\bullet\}$ ,

$$X_1 = \mathcal{F}\{x_1\}, E_1 = \mathcal{F}\{e_1\},$$
 (3)

<sup>&</sup>lt;sup>5</sup>Although [19] includes 5G NR PHY layer abstraction for UL/DL, new NR SL features such as the data and control multiplexing structure for PSCCH/PSSCH [20] lead to link-level performance differences between SL and UL/DL.

<sup>&</sup>lt;sup>6</sup>The slot duration  $s_t$  is determined by NR Numerology  $\mu$ , i.e.,  $t_s = 2^{-\mu}$  ms.

 $<sup>^7{\</sup>rm The}$  supported link simulations for NR SL are conducted with disabled Doppler shift, and TB transmissions see independent channel realizations.

#### Offline link simulation (Performed once per PHY setup)

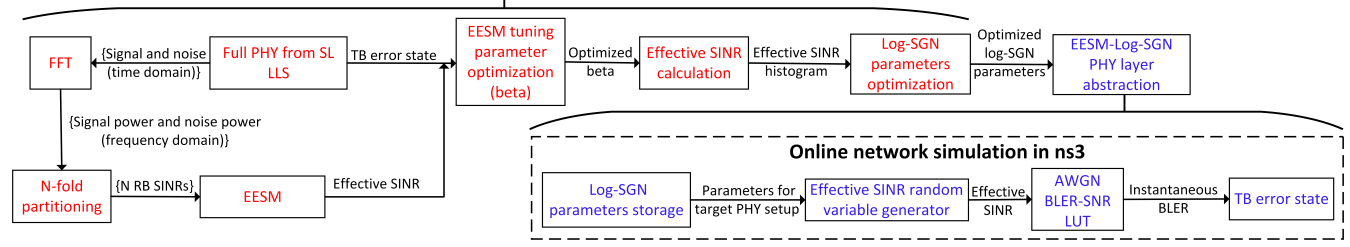


Figure 2: Flowchart of Implementing the PHY Layer Abstraction for 5G NR SL

where  $x_1$  and  $e_1$  denote the signal and noise components within one TB in the time domain, respectively, that is available from the link simulator.  $X_1$  and  $E_1$  denote the corresponding signal and noise components in the frequency domain. Thereafter,  $X_1$  and  $E_1$  are filtered according to the RB allocation structure (depending on numerology and sub-carrier spacing) to obtain the sub-channel  $X_{1,n}$  and  $E_{1,n}$  where  $n \in \mathcal{N}$ . Using Parseval's theorem [12] on conservation of power in time and frequency domains, we have:

$$\sum_{m=1}^{L} |x_1[m]|^2 = \frac{1}{L} \sum_{k=1}^{L} |X_1[k]|^2 = \sum_{n=1}^{|\mathcal{N}|} S_{1,n}, \tag{4}$$

$$\sum_{m=1}^{L} |e_1[m]|^2 = \frac{1}{L} \sum_{k=1}^{L} |E_1[k]|^2 = \sum_{n=1}^{|\mathcal{N}|} N_{1,n}, \tag{5}$$

where the signal and noise sequences in the time and frequency domains are of the same FFT size of length L. In the NIST simulator, the signal or noise sequence length for each TB (FFT size) for numerology  $\mu=0$  is  $L=12600^{-8}$ . within 1 ms time slot, which corresponds to 12.6 MHz sampling rate for the base-band signal. The number of RBs is N=10, where each RB for  $\mu=0$  spans  $12\times15$ kHz = 180 kHz. The time-domain signal and noise sequences of L samples in a TB are transformed into L equally spaced frequency-domain components. As there are N RBs allocated in the frequency domain, we thereby evenly partition the non-zero frequency-domain components into N subsets, where each subset represents one RB.

An L2S mapping function <sup>9</sup> then compresses the post-processing SINRs on different RBs and streams into a single metric called effective SINR, which would yield the same instantaneous BLER for a fading channel with a specific CQI/MCS if the simulation was run for an AWGN-SISO channel with the same CQI/MCS. In this work, we adopt the Exponential Effective SINR Mapping (EESM) to calculate the effective SINR given the post-processing SINRs of each TB. The effective SINR using EESM for the single layer transmission is [9, 19]:

$$SINR_{eff} = -\beta \ln \left( \frac{1}{|\mathcal{N}|} \sum_{n \in \mathcal{N}} \exp(-\frac{SINR_{1,n}}{\beta}) \right), \tag{6}$$

where  $\beta$  is a parameter that needs to be optimized, which characterizes the relation between the target fading channel and the AWGN-SISO channel. It should be noted that the correlation also exists in

the frequency domain (i.e., in the RB level) under the frequency-selective channel. Eq. (6) tries to lose the details of the correlation among the RB SINRs of each TB transmission by compressing them into a single metric-effective SINR.

The effective SINR indicated by Eq. (6) and the associated binary TB error state are determined by the full PHY simulation from the 5G NR SL link simulator. Then the set of effective SINRs and binary TB error states are provided as inputs for optimizing the EESM tuning parameter  $\beta$  so that the Mean Square Error (MSE) between the instantaneous BLER-effective SINR curve for the simulated frequency-selective fading channel and the instantaneous BLER-SNR curve under the AWGN-SISO channel is minimized. The MSE function is expressed as:

$$\beta_{\text{opt}} = \underset{\beta}{\operatorname{argmin}} \frac{1}{|\eta|} \sum_{k \in \eta} |\text{BLER}_r(\text{SINR}_{\text{eff},k}(\beta)) - \text{BLER}_{AWGN}(\text{SINR}_{\text{eff},k}(\beta))|^2,$$
(7)

where all effective SINRs after EESM can be categorized into a set of bins (represented by set  $\eta$ ) where the bin effective SINR of the kth bin is SINR<sub>eff,k</sub>( $\beta$ ). The term BLER<sub>AWGN</sub>(SINR<sub>eff,k</sub>( $\beta$ )) represents the BLER corresponding to the kth bin effective SINR under AWGN-SISO channel, and BLER<sub>r</sub>(SINR<sub>eff,k</sub>( $\beta$ )) is the BLER corresponding to the kth bin effective SINR, which is calculated as:

$$BLER_r(SINR_{eff,k}(\beta)) = \frac{1}{|\zeta_k|} \sum_{l \in \mathcal{L}} \mathbb{1}_{error}(\mathbf{H}_l), \tag{8}$$

where  $\mathbf{H}_l$  represents one of channel realizations falling into the kth bin (represented by the set  $\zeta_k$ ).  $\mathbb{1}_{error}(\mathbf{H}_l)$  is the indicator function of error TB received under the channel realization  $\mathbf{H}_l$ . Once the tuning is complete, the effective SINR of all channel realizations can be updated based on  $\beta_{opt}$ , i.e.,  $\mathrm{SINR}_{eff}(\beta_{opt})$  for each channel realization.

The updated effective SINRs for each SNR point in the full PHY form a histogram which is then statistically fitted with a log-SGN distribution characterized by 4 parameters [16]:

$$X \triangleq \ln(\text{SINR}_{\text{eff}}(\beta_{opt})) \sim \text{SGN}(\hat{\mu}, \hat{\sigma}, \hat{\lambda}_1, \hat{\lambda}_2), \tag{9}$$

with the probability density function (PDF):

$$f_X(x; \hat{\mu}, \hat{\sigma}, \hat{\lambda}_1, \hat{\lambda}_2) = \frac{2}{\hat{\sigma}} \psi \left( \frac{x - \hat{\mu}}{\hat{\sigma}} \right) \Psi \left( \frac{\hat{\lambda}_1(x - \hat{\mu})}{\sqrt{\hat{\sigma}^2 + \hat{\lambda}_2(x - \hat{\mu})^2}} \right), x \in \mathbb{R},$$
 (10)

<sup>&</sup>lt;sup>8</sup>For  $\mu = 1$ , L = 25200.

<sup>&</sup>lt;sup>9</sup>L2S mapping function is a mandatory step in the PHY layer abstraction implementation, which summarizes the effect of possible multiple SNRs affecting the packet by modeling the link as an equivalent AWGN channel.

Communication system	5G NR SL	
Link simulator	NIST 5G NR SL link simulator	
Number of realizations at each SNR	40000	
Channel model	Pedestrian-B [14]	
Channel coding	LDPC	
Number of RBs	10	
CQI (MCS)	6 (8)	
Numerology	0	
SNR points	{2.0, 4.4, 6.8, 9.2, 11.6, 14.0, 16.4}	
Channel estimation error	Noise-free	
CPU	Intel Core i7 CPU at 2.60GHz	

Table 2: Main PHY Layer Setup

where  $\hat{\mu} \in \mathbf{R}$  is the location parameter that characterizes the mean of the obtained histogram.  $\hat{\sigma} > 0$  is the scaling factor,  $\hat{\lambda}_1 \in \mathbf{R}$  and  $\hat{\lambda}_2 \geq 0$  are shape parameters,  $\psi(x)$  is the standard normal PDF, and  $\Psi(x)$  is the standard normal cumulative distribution function. Finally, the corresponding log-SGN parameters are stored via LUTs for use in network simulations.

It should be noted that the link simulation used to generate log-SGN parameters for each PHY setup is offline and performed only once. Network simulation is performed by directly using the stored log-SGN parameters for the target PHY setup. Figure 2 shows the procedures for the online network simulation in ns-3. When running each TB in a network simulator, a realization of SGN distributed X can be generated from a random variable generator for log-SGN PDF using the stored parameters  $\hat{\mu}$ ,  $\hat{\sigma}$ ,  $\hat{\lambda}_1$ ,  $\hat{\lambda}_2$  as inputs. The realization of X is then used to calculate SINR<sub>eff</sub> =  $\exp(X)$ . Then, the effective SINR SINR<sub>eff</sub> is mapped into an instantaneous BLER using the instantaneous BLER-SNR lookup table under the AWGN-SISO channel at the specified TB size, channel code, and CQI (MCS).

# 3 SIMULATION RESULTS

In this section, we validate the efficient PHY layer abstraction using EESM-log-SGN p.d.f curve fitting. Table 2  $^{10}$  shows the PHY setup for the validation of an example case.

We first validate that the optimal  $\beta$  is able to accurately map the characteristics of fading channel to that of the AWGN channel. Figure 3 demonstrates that the instantaneous BLER-effective SINR curve of fading channel under EESM L2S mapping with the optimal  $\beta$  fits the instantaneous TB BLER-SNR curve (lookup table) for AWGN-SISO channel. In this instance, the AWGN-SISO curve shows the relationship between the input SNR and resulting instantaneous BLER from full PHY AWGN-SISO simulations conducted at 0.25dB SNR increments. The EESM points show the relationship between the effective SNRs on every 0.25dB bins and the full PHY simulated instantaneous BLER in each bin. The instantaneous BLERs following those on the AWGN-SISO curve indicate that we can successfully predict instantaneous BLERs using the effective SNRs and AWGN-SISO lookup table.

Afterward, an effective SINR histogram can be obtained based on the post-processing SINRs of each TB under all channel realizations (at one SNR point) and the optimal  $\beta$ , which was shown in Figure 4.

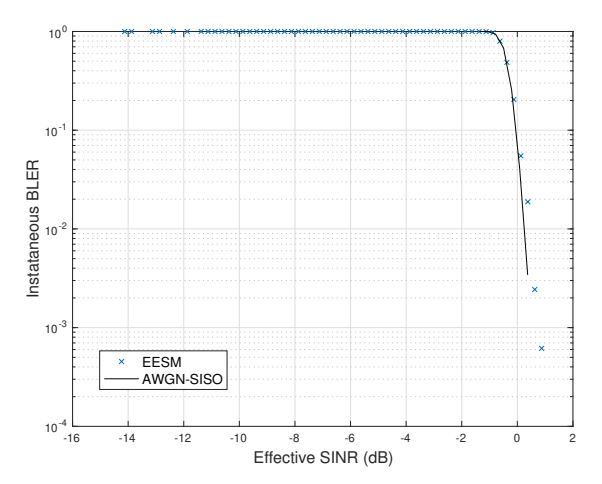


Figure 3: Validation of EESM  $\beta$  Calibration

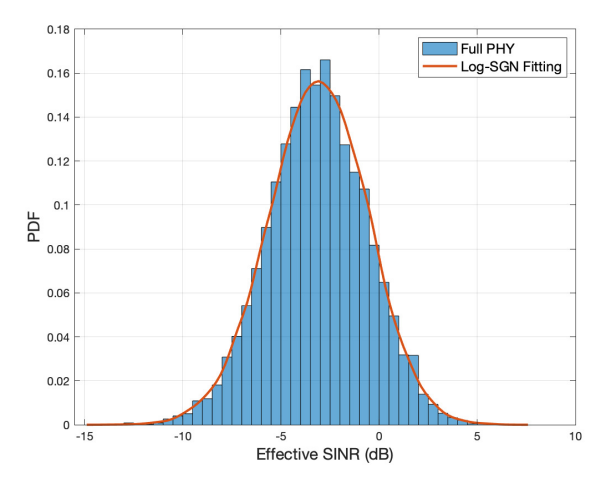


Figure 4: Effective SINR Histogram under SNR = 2

Then the effective SINR histogram is statistically fitted with the log-SGN distribution by Eq. (10). Since the log-SGN fitting curve matches well with the effective SINR histogram, the log-SGN parameters stored in ns-3 LUTs accurately capture the characteristics of the PHY setup in Table 2. The log-SGN parameters of the PHY layer setup at other SNRs are shown in Table 3. The higher the SNR is, the larger the mean  $(\hat{\mu})$  and the scaling factor  $(\hat{\sigma})$  of the corresponding log-SGN distribution.

We then cross-validate the obtained EESM-log-SGN PHY abstraction by comparing its average TB BLER with that from the Full PHY simulation under the same SNR points, which is shown in Figure. 5. We executed 40000 realizations for each SNR point under both methods. Since the average BLER at each SNR point from the EESM-log-SGN PHY abstraction matches well with that from the full PHY, the EESM-log-SGN PHY abstraction for NR SL under the given PHY setup can be verified. Notice that Figure 5 shows the cross-validating experimental data against a processed version of itself. The details of the symbol-level performance in the full PHY can be lost by reducing to i.i.d. log-SGN variables, but the applied

 $<sup>^{10}\</sup>mathrm{The}$  CQI selection is only configured in the NIST 5G NR SL link simulator for the PHY setup. Hence, we associate the CQI with the corresponding MCS based on the 3GPP standard [3].

Table 3: Log-SGN Parameters with CQI 6 (MCS 8)

	O		~	`
SNR	μ̂	σ̂	$\hat{\lambda_1}$	$\hat{\lambda_2}$
2.0	-0.9403	0.6194	0.5727	0.1661
4.4	-0.6545	0.6634	0.9407	0.0939
6.8	-0.3791	0.7273	1.5644	0.3165
9.2	-0.1116	0.8029	2.2530	0.5263
11.6	0.1107	0.9158	3.0635	0.7346
14.0	0.3597	1.0294	3.4050	0.4942
16.4	0.6855	1.1506	3.0456	0.0022

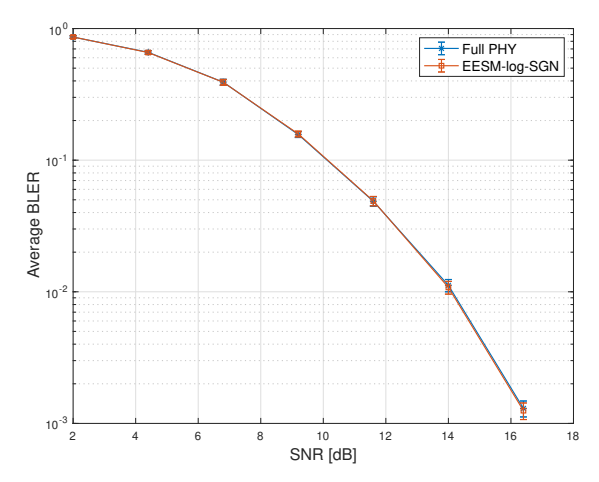


Figure 5: Cross Validation Regarding the Average TB BLER

Table 4: Average Runtimes at One SNR Point over 10 Trials

# of TBs	Numerology	# of RBs	EESM-log-SGN
40000	0	10	0.6 sec
40000	0	20	0.6 sec
40000	1	10	0.6 sec
40000	1	20	0.6 sec
80000	0	10	1.2 sec
80000	0	20	1.2 sec
80000	1	10	1.2 sec
80000	1	20	1.2 sec

EESM-log-SGN method does not lose the fidelity of the packet-level performance metrics such as the BLER. It should be noted that the runtime at each SNR point under the EESM-log-SGN method only takes around 0.6 seconds for the 40000-TB and 1.2 seconds for the 80000-TB simulation, as is shown in Table 4. The runtimes under the EESM-log-SGN method do not scale with Numerology and the number of RBs. Therefore, we do not have to build increasingly complex channel realizations within ns-3, which can achieve fast simulations for 5G NR SL in ns-3.

We further cross-validate the possible temporal correlations by investigating the auto-correlation of the effective SINRs aimed at the same SNR point under two methods, which is shown in Figure 6. The auto-correlation function (ACF) of an autoregressive modeling  ${\rm AR}(p)$  process becomes approximately to 0 after the lag p=0 under the full

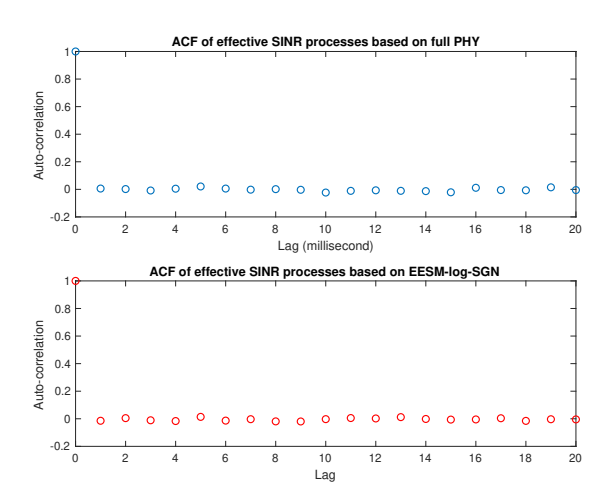


Figure 6: Cross Validation Regarding the Possible Temporal Correlation: ACF of Effective SINR (SINR $_{eff}$ ) Processes under SNR = 2.0

Table 5: Optimal  $\beta$  under Different CQI (MCS) and Numerology

$\mu = 0$	$\mu = 1$
0.5527	0.8360
0.5632	0.9242
0.5578	0.8642
0.5747	0.9125
0.6033	1.0043
0.5988	1.0952
0.9286	1.8323
1.8635	3.1353
3.0324	5.2644
4.3438	7.3591
5.9274	10.4613
8.0815	14.1499
9.5974	18.0639
11.625	24.2971
	0.5527 0.5632 0.5578 0.5747 0.6033 0.5988 0.9286 1.8635 3.0324 4.3438 5.9274 8.0815 9.5974

PHY, which further verifies that the simulated channel instances are independent, i.e., no temporal correlation among channel instances in the currently supported full PHY simulations. While the ACF of an AR(p) process under EESM-log-SGN shows the same results because of the generated i.i.d. log-SGN random variables.

In addition, we investigate the impact of CQI (MCS) and NR numerology  $\mu$  on the optimal  $\beta$  under the same number of RBs indicated in Table 2. Our observation for NR SL is different from that in [19] which uses the PHY layer abstraction for NR Uplink/Downlink. First, unlike the claim in [19] that the optimal  $\beta$  is insensitive to NR numerology for Uplink/Downlink, we observe clear sensitivity to NR numerology for SL, especially for high CQI (MCS) values. Second, under the same numerology, the optimal  $\beta$  is insensitive to CQI (MCS) value when it is less than or equal to 6 (8). Third, under the same CQI (MCS), the optimal  $\beta$  under  $\mu$  = 1 is always greater than that under  $\mu$  = 0, suggesting that higher numerology leads to a larger calibration scale.

#### 4 CONCLUSION AND FUTURE WORK

In this paper, we deployed the EESM-log-SGN PHY layer abstraction framework from [16] for 5G NR SL for OFDM unicast single layer transmission over i.i.d. frequency-selective channels, which is the first PHY layer abstraction work on 5G NR SL. The obtained EESM-log-SGN PHY layer abstraction is verified to achieve good accuracy in modeling the PHY performance for the investigated scenarios while runtimes are significantly reduced compared with the corresponding full PHY simulation. We further explored the impact of CQI (MCS) and NR numerology ( $\mu$ ) on the optimal  $\beta$  in NR SL, and noted differences from corresponding results in NR UL/DL by [19].

Future work may focus on the following directions to develop a more sophisticated PHY layer abstraction for 5G NR SL: 1) Exploring the impact of the number of RBs (i.e., varying TB size) on the optimal  $\beta$ , since here we only investigated the impact of Numerology for the same number of RBs allocated (i.e., TB size is fixed). 2) Exploring the impact of FFT dimension of L on RB's SNR and  $\beta$  in EESM method. 3) Considering the time-varying channels where temporal correlation exists due to Doppler shift rendered by UE's mobility: this direction requires us to further develop the NIST NR SL link simulator by configuring the Doppler shift in the full PHY. The EESM-log-AR method [15] is the preferred option to deal with such a case. 4) Incorporating multiple TB re-transmission [11, 19] that will require new suitable L2S mapping. 5) Finally, extending the NR SL PHY abstraction to multiple streams (maximum number can be up to 2 per [3]).

## **ACKNOWLEDGMENTS**

The authors thank Chunmei Liu and Peng Liu (National Institute of Standards and Technology) as well as Tom Henderson (University of Washington) for insightful technical discussions and guidance throughout the project.

## REFERENCES

- [1] 3GPP. 2014. Study on LTE Device to Device Proximity Services; Radio Aspects (Release 12). Technical Report (TR) 36.843. 3rd Generation Partnership Project (3GPP).
- [2] 3GPP. 2019. Study on NR Vehicle-to-Everything (V2X). Technical Report TR38.885. The 3rd Generation Partnership Project (3GPP).
- [3] 3GPP. 2020. NR; Physical Layer Procedures for Data (Release 16). Technical Specification (TS) 38.214. 3rd Generation Partnership Project (3GPP). https://portal.3gpp.org/desktopmodules/Specifications/SpecificationDetails. aspx?specificationId=3216
- [4] 3GPP. 2021. NR; Physical Channels and Modulation (Release 16). Technical Specification (TS) 38.211. 3rd Generation Partnership Project (3GPP).

- [5] 3GPP. 2021. NR; User Equipment (UE) Radio Transmission and Reception; Part 2: Range 2 Standalone. Technical Specification (TS) 38.101-2. 3rd Generation Partnership Project (3GPP).
- [6] 3GPP TS38.101-1. 2021. 3rd Generation Partnership Project; Technical Specification Group Radio Access Network; NR; User Equipment (UE) Radio Transmission and Reception; Part 1: Range 1 Standalone. Standard. 3GPP.
- [7] 3GPP TS38.212. 2021. 3rd Generation Partnership Project; Technical Specification Group Radio Access Network; NR; Multiplexing and Channel Coding. Standard. 3CPP
- [8] 3GPP TS38.213. 2021. 3rd Generation Partnership Project; Technical Specification Group Radio Access Network; NR; Physical Layer Procedures for Control. Standard. 3GPP.
- [9] Karsten Brueninghaus, David Astely, Thomas Salzer, Samuli Visuri, Angeliki Alexiou, Stephan Karger, and G-A Seraji. 2005. Link Performance Models for System Level Simulations of Broadband Radio Access Systems. In 2005 IEEE 16th International Symposium on Personal, Indoor and Mobile Radio Communications, Vol. 4. Berlin, Germany, 2306–2311.
- [10] Liu Cao, Lyutianyang Zhang, Sian Jin, and Sumit Roy. 2023. Efficient MIMO PHY Abstraction with Imperfect CSI for Fast Simulations. IEEE Wireless Communications Letters (2023).
- [11] Antonio Maria Cipriano, Raphael Visoz, and Thomas Salzer. 2008. Calibration Issues of PHY Layer Abstractions for Wireless Broadband Systems. In 2008 IEEE 68th Vehicular Technology Conference. Calgary, Canada, 1–5.
- [12] Philippe Dennery and André Krzywicki. 2012. Mathematics for Physicists. Courier Corporation.
- [13] Roger Pierre Fabris Hoefel and Oscar Bejarano. 2016. On Application of PHY Layer Abstraction Techniques for System Level Simulation and Adaptive Modulation in IEEE 802.11ac/ax Systems. Journal of Communication and Information Systems 31, 1 (2016).
- [14] ITU-R. 1997. Rec. ITU-R M.1225 Guidelines for Evaluation of Radio Transmission Technologies for IMT-2000. Technical Report. https://www.itu.int/rec/R-REC-M 1225
- [15] Sian Jin, Sumit Roy, and Thomas R Henderson. 2021. EESM-log-AR: An Efficient Error Model for OFDM MIMO Systems over Time-varying Channels. In *Proceedings* of the 2021 Workshop on ns-3. Virtual Event, USA, 17–24.
- [16] Sian Jin, Sumit Roy, and Thomas R Henderson. 2021. Efficient PHY Layer Abstraction for Fast Simulations in Complex System Environments. *IEEE Transactions on Communications* 69, 8 (2021), 5649–5660.
- [17] Sian Jin, Sumit Roy, Weihua Jiang, and Thomas R Henderson. 2020. Efficient Abstractions for Implementing TGn Channel and OFDM-MIMO Links in ns-3. In Proceedings of the 2020 Workshop on ns-3. Virtual Event, USA, 33–40.
- [18] Florian Kaltenberger, Imran Latif, and Raymond Knopp. 2013. On Scalability, Robustness and Accuracy of Physical Layer Abstraction for Large-scale Systemlevel Evaluations of LTE Networks. In 2013 Asilomar Conference on Signals, Systems and Computers. Pacific Grove, USA, 1644–1648.
- [19] Sandra Lagen, Kevin Wanuga, Hussain Elkotby, Sanjay Goyal, Natale Patriciello, and Lorenza Giupponi. 2020. New Radio Physical Layer Abstraction for Systemlevel Simulations of 5G Networks. In 2020 IEEE International Conference on Communications (ICC). Dublin, Ireland, 1–7.
- [20] Peng Liu, Chen Shen, Chunmei Liu, Fernando J Cintrón, Lyutianyang Zhang, Liu Cao, Richard Rouil, and Sumit Roy. 2022. 5G New Radio Sidelink Link-Level Simulator and Performance Analysis. In Proceedings of the 25th International ACM Conference on Modeling Analysis and Simulation of Wireless and Mobile Systems. Montreal, Canada, 75–84.
- [21] Rohan Patidar, Sumit Roy, Thomas R Henderson, and Amrutha Chandramohan. 2017. Link-to-system Mapping for ns-3 Wi-Fi OFDM Error Models. In Proceedings of the 2017 Workshop on ns-3. Porto, Portugal, 31–38.
- [22] Eldad Perahia and Robert Stacey. 2013. Next Generation Wireless LANs: 802.11n and 802.11ac. Cambridge university press.